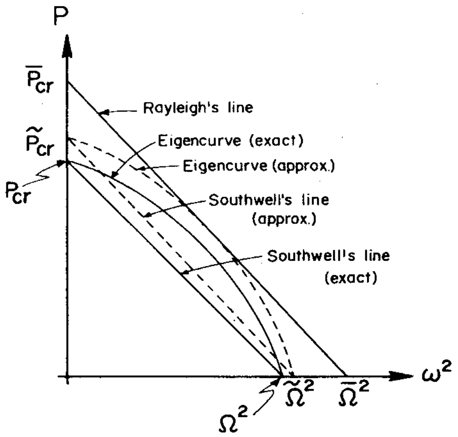

Fig. 2 Load vs frequency square curves based on approximate free vibration and buckling modes.

may be used in the procedure just discussed. However, the straight line joining the approximate natural frequency square $\tilde{\Omega}^2$ and approximate buckling load $\tilde{P}_{cr}$, obtained using the approximate modes, will no longer be a lower bound (Fig. 2); but the Rayleigh line parallel to this line will still be an upper bound.

Example

Consider the vibration and stability of a uniform clamped-clamped beam of length l, subjected to compressive end forces P. Exact values of the fundamental natural frequency and buckling load are

$$\Omega^2 = 500.564EI/\mu l^4$$

and (14)

$$P_{cr} = 4\pi^2 EI/l^2$$

where E = Young's modulus of elasticity, I = moment of inertia of the cross section, and μ = mass per unit length. The vibration and buckling modes are

$$\phi(x) = \left(\cosh\frac{\lambda x}{l} - \cos\frac{\lambda x}{l}\right) - \beta\left(\sinh\frac{\lambda x}{l} - \sin\frac{\lambda x}{l}\right) \tag{15}$$

and

$$\psi(x) = [1-\cos(2\pi x/l)]$$

where $\lambda l = 4.73004$ and $\beta = 0.9825022$. The total energy of the system, similar to Eq. (2), is

$$E = \int_o^l (EIu''^2 - Pu'^2 - \mu\omega^2 u^2)\,dx \tag{16}$$

where $'$ denotes differentiation with respect to x. The coefficients $f_1, f_2 \ldots h_3$, defined in Eq. (6), are obtained using Eq. (16) as

$$\begin{aligned} f_1 &= EI\int_o^l \phi''^2\,dx, & f_2 &= 2EI\int_o^l \phi''\psi''\,dx & f_3 &= EI\int_o^l \psi''^2\,dx \\ g_1 &= -\int_o^l \phi'^2\,dx, & g_2 &= -2\int_o^l \phi'\psi'\,dx, & g_3 &= -\int_o^l \psi'^2\,dx \\ h_1 &= -\int_o^l \phi^2\,dx, & h_2 &= -\int_o^l \phi\psi\,dx, & h_3 &= -\int_o^l \psi^2\,dx \end{aligned} \tag{17}$$

Calculations as indicated in the previous section yield

$$\Delta = 0.00836\,\Omega^2 \tag{18}$$

i.e., an upperbound for the deviation of the eigencurve from the Southwell line is only 0.836% of the natural frequency square.

Conclusions

The method developed in this Note is applicable to any multiple parameter eigenvalue problem, for example, buckling of an elastic structure under multiple independent loadings. For an N-parameter eigenvalue problem, we will obtain two parallel $(N-1)$ degree hyper-surfaces as upper and lower bounds, instead of two parallel lines in the case of the two parameter eigenvalue problem.

References

[1] Lurie, H., "Lateral Vibrations as related to Structural Stability," *Journal of Applied Mechanics*, Vol. 19, 1952, pp. 195–204.

[2] Temple, G. and Bickley, W. G., *Rayleigh's Principle*, Oxford University Press, London, 1933.

[3] Singa Rao, K. and Amba-Rao, C. L., "Lateral Vibration and Stability Relationship of Elastically Restrained Circular Plates," *AIAA Journal*, Vol. 10, No. 12, Dec. 1972, pp. 1689–1690.

[4] Singa Rao, K. and Amba-Rao, C. L., "Comment on 'Lateral Vibration and Stability Relationship of Elastically Restrained Circular Plates'," *AIAA Journal*, Vol. 11, No. 7, July 1973, p. 1056.

[5] Flax, A. H., "Comment on 'Lateral Vibration and Stability Relationship of Elastically Restrained Circular Plates'," *AIAA Journal*, Vol. 11, No. 11, Nov. 1973, pp. 1599–1600.

New Device for Skin-Friction Measurement in Three-Dimensional Flows

RAMESH P. GUPTA*
National Aeronautical Laboratory, Bangalore, India

Nomenclature

D = outer diam of probe tube
d = inner diam of probe tube
p_o = pressure measured by the total head tube of the probe
p_c = pressure measured by the chamfered tube of the probe
p_s = wall static pressure
u_τ = friction velocity $(= [\tau_w/\rho]^{1/2})$
v = kinematic viscosity
ρ = fluid density
τ_w = wall shear stress

I. Introduction

SEVERAL experimental methods are available for measurement of skin-friction. A brief review of these methods is given by Brown and Joubert.[1] A class of these methods is based on the principle of similarity of flow about obstacles. These methods rely on the observation that the flow near the wall is governed by the "wall variables." According to this principle, the velocity field about an obstacle immersed entirely in the "law of the wall" region is completely determined by the wall variables. The wall variables are surface friction, τ_w, density and kinematic viscosity of fluid, ρ, v, and a characteristic length of obstacle, l. Dimensional reasoning gives that any pressure difference is given by (for details, see Brown and Joubert,[1] p. 742)

$$\Delta p l^2/\rho v^2 = f[\tau_w l^2/\rho v^2] \tag{1}$$

This function can be determined experimentally for a given device. Many designs of devices based on this principle are available, such as the Preston-tube,[2–4] Sublayer fence,[5,6] Stanton tube or razor-blade technique,[7,8] Static hole pair[9] etc. It is to be noted here that in all of these methods one of the pressures to be measured is invariably the wall pressure. By contrast, the new device given in this work does not require a wall tapping at the point of measurement. Provision of wall static

Received May 8, 1974; revision received July 10, 1974.
Index categories: Boundary Layers and Convective Heat Transfer – Turbulent; Subsonic and Transonic Flow.

* Scientist, Aerodynamics Division.

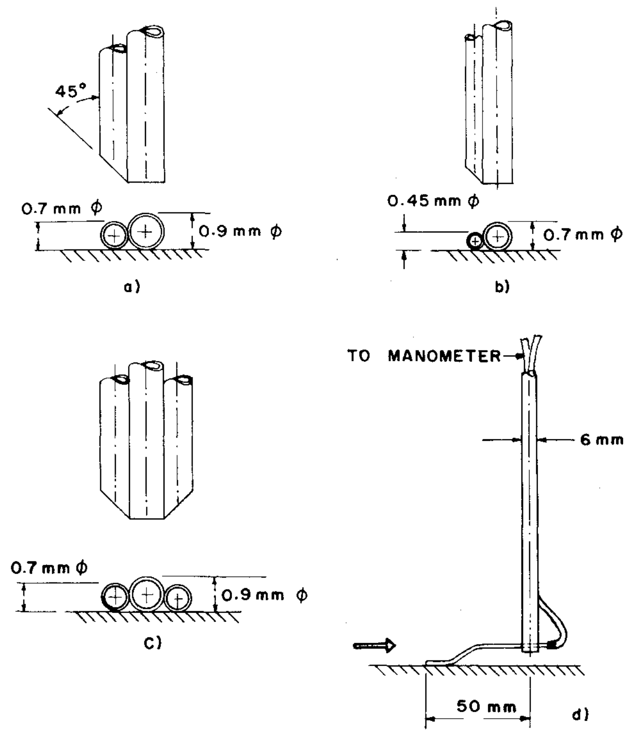

Fig. 1 New device for skin-friction measurement.

tap at many locations of interest may be impracticable, e.g., near the trailing edge of a thin airfoil model. Also, large number of wall taps on a surface specially in a three-dimensional flow where skin-friction changes from point to point cannot be provided, e.g., on a wing model in a wind tunnel. Moreover, surface flow visualization using a mixture of powder and oil on a surface with static wall taps is not advisable as the flowing powder may block the holes. Thus, as the present design does not need measurement of wall pressure, it is expected to be a potential tool for skin-friction measurement in many additional situations where other devices are impracticable.

II. Description of the Device

The device consists of a pair of stainless steel tubes with different diameters placed side by side on the surface to face the flow (Figs. 1a and b). The tube with smaller diameter is chamfered side way (at 45° in this work) to increase the measured pressure difference and thus to increase the accuracy of measurement. The tubes are so arranged that both of them can touch the wall surface simultaneously. Two different combinations of the larger and smaller diameters of the tubes were used as shown in Figs. 1a and 1b. The alternate design given in Fig. 1c is suitable for three-dimensional flows. In this case an additional chamfered tube with same chamfer angle and same inner and outer diameters is added symmetrically. This device is first used as a Conrad probe to align the probe in the local flow direction on the surface in a three-dimensional flow. Then the pressure difference $(p_o - p_c)$ between the central tube and the chamfered tube is used as a measure of skin-friction with a suitable calibration curve similar to a Preston tube. The over-all design and dimensions of the device is shown in Fig. 1d. The ratio (d/D) for all the tubes in the device was approximately 0.6. A flattened total head tube was also used for velocity profile measurements and to ascertain whether the boundary-layer was laminar or turbulent.

III. Experimental Set-Up

A low-speed suction type wind tunnel (max. speed 30 m/sec, test section: 30 cm height and 13 cm wide) was used for this study. The side wall on which the measurements were made was 3 mm thick perspex sheet with a static wall tap. A sandpaper strip, just upstream of test-section, in the contraction on the side wall was used for early transition. Least count of traverse for velocity profile survey was 0.125 mm. A well-type manometer with a least count of 0.125 mm of alcohol was used for this study. The dimensions of various tubes in the device are given in Fig. 1. Experiments were done for five freestream dynamic heads, and each time the pressure difference $(p_o - p_c)$ was measured for both the devices (Table 1). A velocity profile survey with the flattened total head tube was also made for all the dynamic heads. It was seen that the presence of chamfered tube had negligible effect on the reading of total head tube.

Table 1 Pressure measurements by the new device

Device	Dynamic head (cm of al)	$p_o - p_c$ (cm of al)	Preston-tube value (cm of al)	$K = \frac{\text{Preston-tube value}}{(p_o - p_c)}$
	5.42	1.206	1.689	1.400
	4.55	1.004	1.409	1.404
Fig. 1a	3.96	0.851	1.194	1.400
	2.52	0.508	0.711	1.400
	1.90	0.254	0.356	1.400
	5.42	1.245	1.562	1.255
	4.55	1.054	1.321	1.253
Fig. 1b	3.96	0.876	1.092	1.247
	2.52	0.508	0.635	1.250
	1.90	0.242	0.305	1.260

IV. Application of the Device

It is necessary to calibrate the pressure difference $(p_o - p_c)$ obtained by the proposed device against a well-known device, which is here taken to be Preston tube. The Preston tube values $(p_o - p_s)$ and the corresponding values $(p_o - p_c)$ are given in Table 1 for five different dynamic heads. It is seen that the ratio $K = (p_o - p_s)/(p_o - p_c)$ is almost a constant for each of the two devices.

The device is first calibrated in a tunnel against a Preston tube to obtain the calibration constant K. (It is found to be approximately 1.40 and 1.25 for the devices of Figs. 1a and 1b). For the measurement of skin friction at the point of interest, it is necessary now only to measure $(p_o - p_c)$ with the new instrument. The known calibration constant K for the device then gives the corresponding Preston-tube shear value. Well-known calibration curves[4] for the Preston tube then gives the skin friction.

To check the consistency of the measurements, the Preston-tube values of $(p_o - p_s)$ were used to calculate the friction velocity from the tabular values given by Head and Vasanta Ram[10] with a claimed accuracy of better than $\pm 1\%$. These values of friction velocity for two different Preston tubes are given in Table 2 and very good agreement confirms the accuracy of the present measurements.

Velocity profile survey by a flattened total head probe was also done to check the type of the boundary layer. The integral

Table 2 Friction velocity by various methods

Dynamic head (cm of al)	Friction velocity, u_τ (cm/sec) Preston-tube $D = 0.9$ mm	Preston-tube $D = 0.7$ mm	Ludwieg-Tillman formula	Bradshaw's method
5.42	107.0	107.7	112.0	114.0
4.55	100.0	100.5	102.2	103.7
3.96	92.7	92.5	95.0	95.0
2.52	74.6	75.0	77.7	78.6
1.90	56.7	57.0	58.2	58.4

boundary-layer parameters were calculated from this data applying a modified variable step size Simpson's rule using a high-speed computer. This data was then used to calculate the friction velocity using the Ludwieg-Tillman empirical relation. These values, together with the friction velocity obtained by a method suggested by Bradshaw,[11] are also given in the table. The good agreement in the values of friction velocity obtained by various methods further demonstrates the care taken in doing the experiments. The velocity profile data was plotted in "law of the wall" coordinates to check the existence of log law in the overlap region. Also, good agreement with the Clauser's[12] curve amply proved that the boundary layers were fully-developed, zero pressure gradient, two-dimensional, and turbulent. The new device is thus expected to be useful for skin-friction measurements, specially in three-dimensional flows.

References

[1] Brown, K. C. and Joubert, P. N., "The Measurement of Skin-Friction in Turbulent Boundary-Layers with Adverse Pressure Gradients," *Journal of Fluid Mechanics*, Vol. 35, 1969, pp. 737–757.

[2] Preston, J. H., "The Determination of Turbulent Skin-Friction by Means of Pitot Tube," *Journal of the Royal Aeronautical Society*, Vol. 50, 1954, pp. 190–121.

[3] Head, M. R. and Rechenberg, I., "The Preston-tube as a Means of Measuring Skin-Friction," *Journal of Fluid Mechanics*, Vol. 14, 1962, pp. 1–17.

[4] Patel, V. C., "Calibration of Preston-tube and Limitations on its Use in Pressure Gradients," *Journal of Fluid Mechanics*, Vol. 23, 1965, pp. 185–208.

[5] Nash-Waber, J. L. and Oates, G. C., "An Instrument for Skin-friction Measurement in Thin Boundary Layers," *Transactions of the ASME: Journal of Basic Engineering*, Paper 71-FE-27, 1971.

[6] Vagt, J. D. and Fernholz, H., "Use of Surface Fences to Measure Wall Shear Stress in Three-dimensional Boundary Layers," *Aeronautical Quarterly*, Vol. 24, Pt. 2, May 1973, pp. 87–91.

[7] Stanton, T. E., Marshall, D., and Bryant, C. N., "On the conditions at the boundary of a fluid in turbulent motion," *Proceedings of the Royal Society of London*, Ser. A. Vol. 97, 1920, pp. 413–434.

[8] East, L. F., "Measurement of Skin-friction at Low Subsonic Speed by the Razor-blade Technique," ARC RM 3525, 1968, Aeronautical Research Council, London.

[9] Duffy, J. and Norbury, J. F., "The Static Hole Pair as a Skin-friction Meter," *Journal of the Royal Aeronautical Society*, Vol. 71, 1967, pp. 55–56.

[10] Head, M. R. and Vasantaram, V., "Simplified Presentation of Preston-tube Calibration," *Aeronautical Quarterly*, Vol. 22, Pt. 3, Aug. 1971, pp. 295–300.

[11] Bradshaw, P., "A Simple Method for Determining Turbulent Skin-friction from Velocity Profiles," *Journal of the Aerospace Sciences*, Vol. 26, 1959, p. 841.

[12] Clauser, F. H., "Turbulent Boundary Layer in Adverse Pressure Gradient," *Journal of the Aero-Space Sciences*, Vol. 21, 1954, pp. 91–108.

Adjustment to the Shape Factor Reflection Analysis

D. C. Look*
University of Missouri at Rolla, Rolla, Mo.

Nomenclature

S = diffuse component shape factor
T = specular component shape factor
V_o = detecting system dark level
V_D = nonregularly reflected component
V_s = regularly reflected component
V_1 = nonregular reflection amplitude component
V_2 = regular reflection amplitude component
β = total scatter angle = $\psi+\theta$
θ = angle of reflection
ψ = angle of incidence

Superscripts
D = diffuse
s = specular

Received June 5, 1974; revision received August 9, 1974.
Index categories: Thermal Surface Properties; Radiation and Radiative Heat Transfer.

* Associate Professor, Thermal Radiation Transfer Group, Department of Mechanical and Aerospace Engineering. Member AIAA.

Introduction

An empirical expression, presented by the author,[1–3] closely represents the radiant power reflected from surfaces. In Ref. 1, the angular variation of "radiation diffusely reflected" from flat powder aluminum oxide samples was examined. This actual angular variation was not compatible with the ideal diffuse assumption. By introducing a shaping factor, an improved compatibility was obtained. The samples discussed in Ref. 2 were made of brass and were first polished and then roughened to various degrees by glass shot peening. Because these samples exhibited vastly divergent reflection characteristics—some samples were essentially mirrors—the empirical formulation presented in Ref. 1 was insufficient. The author, therefore, deduced the expression, which consists of two shape factor expressions.

Based on the assumption that the regular and nonregular reflection components are summable, this expression consists of a near diffuse portion (nonregularly reflected), which is directly dependent on a shape factor S, and a "glare" or near specular portion (regularly reflected), which is dependent on a shape factor T. The first term corresponds to the nonregularly reflected component that was presented in Ref. 1 and augmented for a particular illumination-detection condition. The second term corresponds to the regularly reflected component. In both Refs. 1 and 2, data were acquired by varying both the angle of incidence and the angle of reflection such that their sum was constant. Both of these angles are measured in the plane of incidence, and the procedure is accomplished by rotating the surface.

To foster additional confidence in the use of the empirical expression, the author acquired additional data in the "usual way" and presented them in Ref. 3. The samples used were the same samples that were used in Ref. 2, and the "usual way" in which the author acquired the data implies that the angle of incidence was held constant while the reflection angle was varied. The empirical expression represents the data quite well. Thus, the angular variations as represented by the expression appear to be correct, because the data, acquired by two different techniques (independent variables), were fit by the expression.

To test the formulation further, the author studied several types of paper, whose surface properties are intermediate between the "diffuse," aluminum oxide surfaces of Ref. 1 and the "roughened mirror," brass surfaces of Refs. 2 and 3. Though each set of acquired data differed slightly, characterized by the type of paper, all the sets indicated upon data reduction that the second term in the empirical expression is inappropriate.

This Note presents the bidirectional reflectance data, typical of most of the papers that were used to correct the expression, particularly, its regular component portion.

Analysis

The empirical expression presented by the author[2,3] is

$$\begin{aligned} V &= V_o + V_D\cos\psi + V_s\cos\psi\cos(\beta-\psi), \qquad o \leq \theta < \theta_m \\ &= V_o + V_D(A/B)\cos(\beta-\psi) + V_s\cos\psi\cos(\beta-\psi) \\ &\qquad\qquad \theta_m \leq \theta \leq \pi/2 \end{aligned} \tag{1}$$

in which

$$\text{and}\quad \begin{aligned} V_D &= V_1[\cos\psi\cos(\beta-\psi)/\cos^2\beta/2]^{S-1} \\ V_s &= V_2[\cos\psi\cos(\beta-\psi)/\cos^2\beta/2]^{T-1} \end{aligned} \tag{2}$$

The parameter θ_m, which can be defined by referring to Fig. 1, is the value of θ such that A' and B' are equal and is the change-over point from the condition of over-illumination [Eq.